ELSEVIER

Polymer 44 (2003) 2957–2964

polymer

www.elsevier.com/locate/polymer

Solid polymer electrolytes V: microstructure and ionic conductivity of epoxide-crosslinked polyether networks doped with $LiClO_4$

Ping-Lin Kuo*, Wuu-Jyh Liang, Ting-Yen Chen

Department of Chemical Engineering, National Cheng Kung University, Tainan 70101, Taiwan, ROC

Received 21 October 2002; received in revised form 27 January 2003; accepted 21 February 2003

Abstract

A crosslinked polyether network was prepared from poly(ethylene glycol) diglycidyl ether (PEGDE) cured with poly(propylene oxide) polyamine. Significant interactions between ions and polymer host have been observed for the crosslinked polyether network in the presence of $LiClO_4$ by means of FT-IR, DSC, TGA, and ^7Li MAS solid-state NMR. Thermal stability and ionic conductivity of these complexes were also investigated by TGA and AC impedance measurements. The results of FT-IR, DSC, TGA and ^7Li MAS solid-state NMR measurements indicate the formation of different types of complexes through the interaction of ions with different coordination sites of polymer electrolyte networks. The dependence of ionic conductivity was investigated as a function of temperature, $LiClO_4$ concentration and the molecular weight of polyether curing agents. It is observed that the behavior of ion transport follows the empirical Vogel–Tamman–Fulcher (VTF) type relationship for all the samples, implying the diffusion of charge carrier is assisted by the segmental motions of polymer chains. Moreover, the conductivity is also correlated with the interactions between ions and polymer host, and the maximum ionic conductivity occurs at the $LiClO_4$ concentration of $[O]/[Li^+] = 15$.

Keywords: Polyether; Polymer electrolyte networks; Ionic conductivity

1. Introduction

Starting from the late 1970s, solid polymer electrolytes (SPE) based on polyether matrixes have attracted considerable attention in the scientific community, especially in the fields of polymer chemistry and physics, solid-state electrochemistry, and energy storage technology. This interest arises from the possibility of applications of polymer ionic conductors in energy storage systems, electrochromic windows, and fuel cells or sensors operating from subambient to moderate temperatures [1–3].

Among the first and most studied host for SPE is poly(ethylene oxide) (PEO), which is a polymer that dissolves high concentrations of a wide variety of salts to form polymeric electrolytes [4]. This conventional ion-conducting polymer has, in general, multiphase nature consisting of a salt-rich crystalline phase with conductivity appreciable only above 65 °C [5], a pure PEO spherulite crystalline phase, and an amorphous phase with dissolved salt. It has been revealed that the ion conduction takes place primarily in the amorphous phase and the phase diagram is affected by many factors, such as the salt species, preparation method, concentration, temperature, and thermal history. At present, amorphous PEO complexes are considered to be suitable for achieving high and stable conductivity [1,6,7]. To improve electrolyte efficiency, various methods have been applied to modify the structure and morphology of polyether hosts. These investigations have been directed towards decreasing the crystallinity and increasing the rate of structural relaxation in the polyether while maintaining good, stable mechanical and electrochemical properties over the entire operational temperature range of the electrolyte.

In our laboratory, the gelled SPEs based on segmented polyurethanes with polyethylene oxide/polydimethylsiloxane [8] and with polyethylene oxide/perfluoropolyether [9] blocks, respectively, as well as crosslinked epoxy-siloxane polymer complexes [10] were previously prepared and investigated. In this study, to stand on practical viability, specifically solvent-free SPEs based on polyether epoxy

* Corresponding author. Tel.: +886-6-275-7575x62658; fax: +886-6-276-2331.

E-mail address: plkuo@mail.ncku.edu.tw (P.L. Kuo).

0032-3861/03/$ - see front matter © 2003 Elsevier Science Ltd. All rights reserved.
doi:10.1016/S0032-3861(03)00189-7

crosslinked with poly(propylene oxide) (PPO) polyamines have been prepared. Systematic characterization studies of the crosslinked polyether networks in the presence of $LiClO_4$ were established with FT-IR, DSC, TGA, ^{7}Li MAS solid-state NMR, and AC impedance measurements. Glass transition temperature, thermal stability, and ionic conductivity are correlated with the structure of the crosslinked polyether networks and interpreted in terms of the properties of polymer networks and the interaction between the ions and polymer networks.

2. Experimental

2.1. Materials

Poly(ethylene glycol) diglycidyl ether (PEGDE; Kyoeisha Chemical Co., Ltd), epoxy monomer, with an equivalent weight of epoxy groups equals to 290 g/equiv., and two PPO polyamines (Jeffamine D400 and D2000, Huntsman Corporation), curing agents, with the equivalent weights of active hydrogen equal to 115 and 514 g/equiv., respectively, were dehydrated at 80 °C under vacuum for 24 h prior to use. Lithium perchlorate ($LiClO_4$; Aldrich) was dried at 120 °C under vacuum for 72 h. Acetone (Alps) and other chemicals were reagent grade and used without further purification.

2.2. Preparation of crosslinked polyether networks and doped with $LiClO_4$

Polymer electrolyte network films of ca. 200 μm thickness were prepared by weighing required amount of epoxy monomer and the stoichiometric amount of curing agent dissolved in acetone, then varying amounts of $LiClO_4$ were added to the above solution and dissolved. The concentration of $LiClO_4$ in the polymer network complexes was represented by the molar ratio of oxygen of polyether segments to $LiClO_4$ ([O]/[Li^+]). After vigorous stirring, the mixture was then poured into aluminum plate, followed by evaporating the solvent at room temperature. It was then transferred to an air-circulating oven at a temperature ranging from 150–185 °C for different time intervals in order to ensure completion of curing before the occurrence of oxidation. These specimens obtained were placed under vacuum at 80 °C for 72 h until no weight loss observed and then transferred into an argon-filled glove box (Vacuum Atmosphere, USA) for cell assembly. The undoped polymer films were also made in the same way without adding $LiClO_4$. IR (KBr, pellet): $\nu = 3660–3350\ cm^{-1}$ (–OH stretching), 2909 and 2871 cm^{-1} ($-CH_2$ and $-CH_3$ stretching), 1080 cm^{-1} (–C–O–C– stretching), and 620 cm^{-1} (ClO_4^- stretching). ^{13}C CP/MAS NMR (ppm): (δ 18 (–O–CH_2–CH(CH_3)–), 53 (–CH_2–N– and –CH(CH_3)–N–), and 72–77 (carbon atoms next to oxygen atoms of the polyether segments).

3. Characterization

3.1. Methods

FT-IR spectra were measured by using a Bio-RAD FTS-40 equipment with a wavenumber resolution of 2 cm^{-1}, and a minimum of 64 scans was signal-averaged at room temperature under dry nitrogen atmosphere. Each sample was prepared by mixing with potassium bromide (KBr) pellet, and films were vacuum-dried at 80 °C for several days to reduce the absorbed water in the sample.

^{13}C CP/MAS, ^{7}Li MAS solid-state NMR experiments were carried out on a Bruker AVANCE 400 spectrometer, equipped with a 7 mm double-resonance probe, operating at resonance frequencies of 100.63 MHz for ^{13}C nucleus, 155.5 MHz for ^{7}Li nucleus, and 400.17 MHz for ^{1}H nucleus, respectively. The acquirement of ^{13}C spectra were obtained by performing the CP/MAS experiments which use Hartmann–Hahn transfer technique and proton decoupling during acquisition to enhance the spectra sensitivity. The recycle delay time was 4 s, the contact time for ^{13}C CP/MAS was 1.5 s and 90° pulse width for ^{1}H excitation was 5.5 μs. The ^{7}Li MAS spectra were measured with 3 μs pulse length, π/2 pulse angle, 2 s recycle delay and high power decoupling. All ^{7}Li NMR spectra were obtained under variable temperature conditions and a MAS rate of 3 kHz. Chemical shifts were externally reference to solid LiCl at 0.0 ppm.

Differential scanning calorimeter (DSC) (Du Pont TA2010) measurements were conducted over the temperature ranges of − 120–150 °C at a heating rate of 10 °C/min under dry nitrogen atmosphere. The samples were first annealed at 150 °C for 10 min, cooled down to − 120 °C and then scanned. All the thermograms are base line corrected and calibrated against Indium metal. The glass transition zone was determined as the temperature range between two intersection points of the base lines with the extrapolated sloping portion of the thermogram, which resulted from a heat capacity change. T_g was defined as the inflection point of the curve.

Thermal stability was determined with a thermogravimetric analyzer (TGA) (Perkin–Elmer TGA 7) over a temperature range of 100–800 °C at a heating rate of 20 °C/min under nitrogen atmosphere.

AC impedance measurements of the polymer electrolytes were performed using thin films prepared previously of about 200 μm in thickness and 0.785 cm^2 in area. The ionic conductivity of all the films sandwiched between two polished stainless steel blocking electrodes was obtained by using Model 604A Electrochemical Analyzer (CH Instruments, Inc., USA) under an oscillation potential of 10 mV from 100 kHz to 10 Hz. The presenting ionic conductivity values are obtained by using the following relationship:

$$\sigma = \frac{1}{R_b} \times \frac{l}{A}$$

where R_b is the intercept of the straight line and real axis in the Nyquist plot, l and A represent the film thickness and surface area of an electrode, respectively.

4. Results and discussion

4.1. IR studies on the polyether networks and doped with $LiClO_4$

In this study, all of the resulted polymer films were transparent and elastic. The schematic structure of polymer networks is shown in Scheme 1. Introduction of a salt in the polymer networks can change the intermolecular interactions. Thus, an IR analysis was carried out to elucidate the predominant micro arrangements present in the polymer electrolyte networks. Fig. 1 shows the FT-IR spectra of PEGDE-D400 and of PEGDE-D400·$LiClO_4$ complexes. PEGDE-D400 shows the characteristic bands for the –OH and –C–O– absorptions at 3660–3350 and 1080 cm^{-1}, respectively, and the absorption peak of epoxide at 912 cm^{-1} (Fig. 1(b)) disappeared indicating the complete reaction of epoxide on PEGDE. The spectra of PEGDE-D400·$LiClO_4$ complexes showed qualitatively a similar profile to that of the salt-free PEGDE-D400, however, the hydroxy group vibrational modes shifted to lower frequencies and the absorption around 1110 cm^{-1} and 620 cm^{-1} were broadened and split. These bands can be assigned to the stretching modes of ClO_4^- [11].

Fig. 1(a) shows the hydroxy stretching bands as a function of $LiClO_4$ concentrations for the PEGDE-D400 polymer networks. A slightly progressive shift in the maximum of OH stretching band to lower wavenumbers with increasing $LiClO_4$ concentration is observed. In addition, a further hydroxyl stretching vibration is detected around 3200 cm^{-1} for each polymer complex network, which can be attributed to the hydroxy groups forming hydrogen bonding clusters with ClO_4^- ions [12]. Changes in FT-IR can be ascribed to the interactions between hydroxy groups and ions. Since an ion-dipole interaction is stronger than a dipole–dipole interaction, a negative shift in the wavenumber takes place. The FT-IR spectra in the range of 1500–500 cm^{-1} relative to the C–O–C asymmetric stretching region for the PEGDE-D400 with different $LiClO_4$ concentrations are shown in Fig. 1(b). It is obvious that the relative intensity of the peak at 620 cm^{-1} increases with the increasing concentration of $LiClO_4$. Moreover, the changes in intensity, shape and position of the C–O–C stretching mode with the increasing $LiClO_4$ concentration are associated with different micro arrangement. Probably, the basic ether oxygens of polyether chains interact with acceptor groups to a greater extent in these polymer networks. A similar trend was observed in our earlier observations of the epoxy-siloxane polymer complexes system [10].

4.2. Transition temperature and thermal stability

Thermal properties of the crosslinked polyether networks undoped and doped with $LiClO_4$ were investigated by DSC and TGA. Fig. 2 shows the DSC thermograms of PEGDE-D400 and of PEGDE-D400·$LiClO_4$ complexes with various $LiClO_4$ concentrations, and the results are complied in Table 1. From Fig. 2, for the PEGDE-D400 polymer

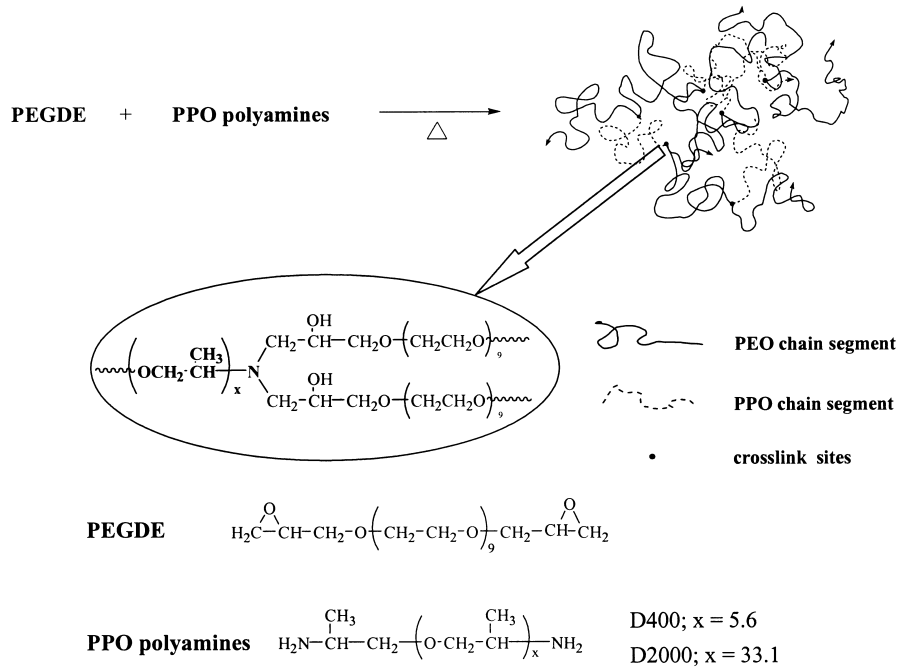

Scheme 1. Schematic structure of polymer networks.

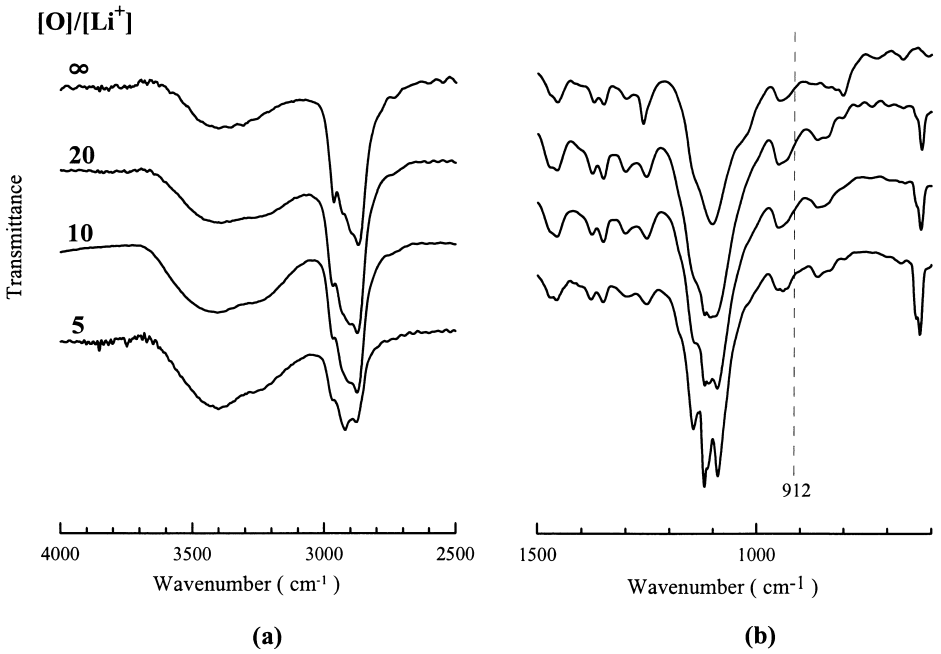

Fig. 1. FT-IR spectra recorded of PEGDE-D400 with various $LiClO_4$ concentrations in the frequency range from (a) 4000 to 2500 cm^{-1}, and (b) 1500 to 500 cm^{-1}.

network, two thermal transition temperatures can be observed at very different temperatures. The lower temperature (T_{g1}) is attributed predominantly to the motion of the polyether segments of the network, and the slight inflection in the range of 35–50 °C (T_{g2}) corresponds to the glass transition temperature of the network above which the chain motion takes place, as observed for usual epoxy polymers [13–15]. Also, no melting transition exists for any of the samples in the range of analyzed temperature, indicating no existence of crystalline structure in polymer networks.

In comparison with the salt-free PEGDE-D400, a significant increase in T_{g1} with increasing $LiClO_4$ concentration is observed. This suggests the formation of complexes between polyether segments and the dissolved $LiClO_4$. Similar behaviors were verified in our recent works for segmented polysiloxane modified polyurethane [8] and epoxy-siloxane polymer network [10] complexed with $LiClO_4$, and were attributed to the formation of transient crosslinks between the salt and the polyether chains. Also, the less obvious inflection of DSC curve in T_{g2} for PEGDE-D400·$LiClO_4$ complexes can be observed. The glass transition zone (ΔT_{g1}) has a maximum value at the $LiClO_4$ concentration of $[O]/[Li^+] = 15$. ΔT_{g1} is defined as the difference between the onset and endset temperatures of glass transition process and reflects the number of relaxation processes associated with the glass transition. Complexed polyether units may be located randomly along the polyether segments. The mutual influences on the behaviors of the free and complexed polyether units probably undergo relaxation processes with different relaxation times, resulting in broadening of the glass transition. At a higher $LiClO_4$ concentration, almost all polyether units are complexed with $LiClO_4$, and thus the distribution of the relaxation times becomes narrow again. The possibility of complex

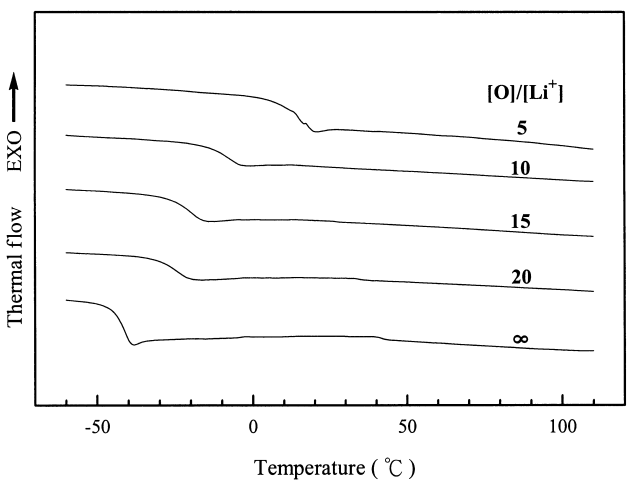

Fig. 2. DSC curves of PEGDE-D400 and PEGDE-D400·$LiClO_4$ complexes with various $LiClO_4$ concentrations.

Table 1
Thermal properties of PEGDE-D400 and PEGDE-D400·$LiClO_4$ complexes

$[O]/[Li^+]$	T_{g1} [a] (°C)	ΔT_{g1} (°C)	$T_d^{0.1}$ [b] (°C)
∞	−41.2	5.1	383
20	−24.5	10.6	310
15	−19.8	10.7	314
10	−7.8	10.2	311
5	14.7	7.7	300

[a] The glass transition temperature measured by DSC.
[b] The temperature for 10% weight loss measured by TGA.

formation between polyethers and alkali metal salts is fundamental for obtaining good polymer electrolytes.

Thermogravimetric analysis (TGA) is used to measure the thermal stability of polymer networks. Fig. 3 shows the weight loss behaviors of the undoped and $LiClO_4$ doped PEGDE-D400 polymer networks investigated by TGA scanning from 100 to 800 °C under nitrogen. As can be seen from Fig. 3, the salt-free polymer network decomposes in a single step and the temperature of initial 10% weight loss ($T_d^{0.1}$) occurs at around 383 °C. The introduction of salt promotes the creation of a second stage which reflects the salt/polymer complex degradation and their $T_d^{0.1}$ takes place at 300–314 °C. This behavior may be explained by the weakness of C–O bond, caused by the electronic density decreasing due to the O–Li^+ interaction. Alternatively, perchlorate oxidation of polyether phase can cause this thermal event starting from ~600 °C.

4.3. ^{7}Li MAS solid-state NMR measurements

^{7}Li MAS solid-state NMR was used to acquire further information from the interactions of Li^+ ions with polymer hosts. The NMR line widths decrease significantly as the proton decoupling was applied on acquiring the ^{7}Li MAS NMR spectra, as reported in our earlier work [16]. This implies that there is a significant ^{7}Li–^{1}H dipolar interaction of Li^+ ions with polymer backbones. Fig. 4 shows the variable temperature ^{7}Li proton-decoupled MAS NMR spectra for PEGDE-D400·$LiClO_4$ complexes at the $LiClO_4$ concentration of $[O]/[Li^+] = 15$. At lower temperature, two distinct resonances become well resolved. For instance, two signals at −0.16 ppm (site I) and at −0.91 ppm (site II) are observed at 213 K, indicating that there exist at least two inequivalent ^{7}Li quadrupole interactions and the accompanied two distinct local environments existing in the polymer complexes. Spinning sidebands are also observed at low temperature, indicating that ^{7}Li quadrupole interaction is increased due to the decrease in lithium

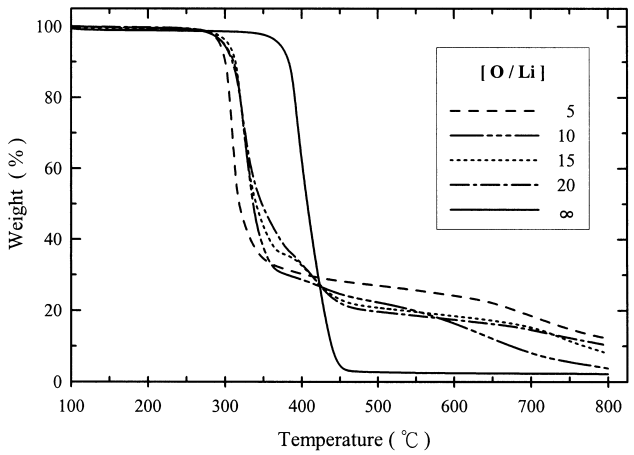

Fig. 3. TGA thermograms of PEGDE-D400 and PEGDE-D400·$LiClO_4$ complexes with various $LiClO_4$ concentrations under nitrogen atmosphere.

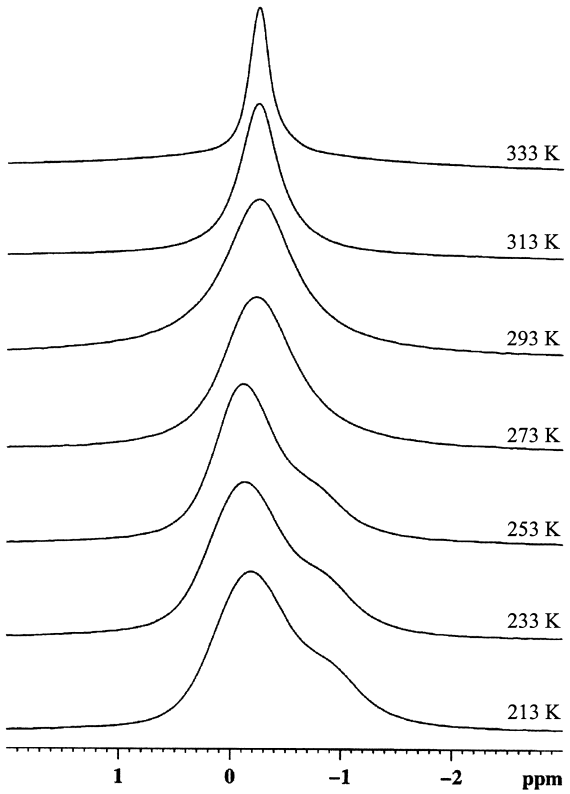

Fig. 4. ^{7}Li proton-decoupled MAS NMR spectra of PEGDE-D400·$LiClO_4$ complexes under various temperatures at the $LiClO_4$ concentrations of $[O]/[Li^+] = 15$.

mobility with decreasing the temperature. As the temperature is raised, the two resonances begin to shift and eventually coalesce into a single resonance. This is the classical peak in a two-site exchange process. At the temperature above 313 K, cation exchange is fast in comparison to the NMR time scale, resulting in a single resonance with a chemical shift that is a weighted average of the individual components and the chemical shift difference between two sites.

Fig. 5 shows the ^{7}Li proton-decoupled MAS NMR spectra for PEGDE-D400·$LiClO_4$ complexes as a function of $LiClO_4$ concentration, recorded at 213 K. At the doping level of $[O]/[Li^+] = 20$ (Fig. 5(a)), the intensity of site I is significantly larger than that of site II, indicating that the Li^+ ions is preferentially coordinated to site I. The intensity of site II increases with increasing salt concentration, where the intensity of site I is normalized, and a shoulder (site III) becomes visible at lower frequency. Since site III is only observed at high salt concentration and shows a concentration dependence of its chemical shift, site III is assigned to the ion pairs or aggregates. It is reasonable to assume that as site I is saturated, then the excess Li^+ ions are coordinated to site II. More and more Li^+ ions are residing in site III as ion pairs or aggregates. These observations are consistent with the FT-IR spectra for PEGDE-D400 with various $LiClO_4$ concentrations as shown in Fig. 1(b) and with the DSC results which show a maximum for glass

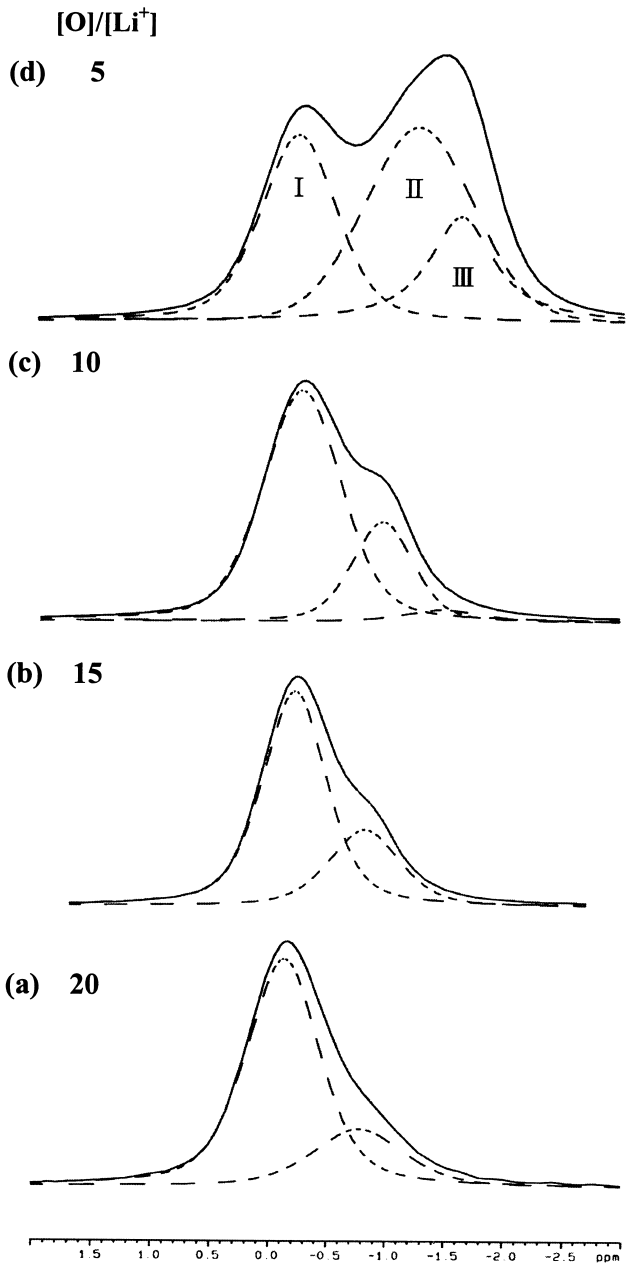

Fig. 5. The deconvolution of ^{7}Li proton-decoupled MAS NMR spectra of PEGDE-D400·$LiClO_4$ complexes as a function of $LiClO_4$ concentration at 213 K.

transition zone at the $LiClO_4$ concentration of $[O]/[Li^+] = 15$. It supports that site II is attributable to the Li^+ ions coordinated to oxygen atoms in the polyether segments. ^{7}Li proton-decoupled MAS NMR spectra for PEGDE-D400·$LiClO_4$ and PEGDE-D2000·$LiClO_4$ complexes with different molecular weight PPO chains of the curing agents at the concentration of $[O]/[Li^+] = 10$ are presented in Fig. 6. It is clearly observed that the intensity of site II relative to that of site I in PEGDE-D400·$LiClO_4$ is significantly less than that of PEGDE-D2000·$LiClO_4$. Except for oxygen atoms in the polyether segments, the Li^+ ions are most possibly coordinated to nitrogen atoms

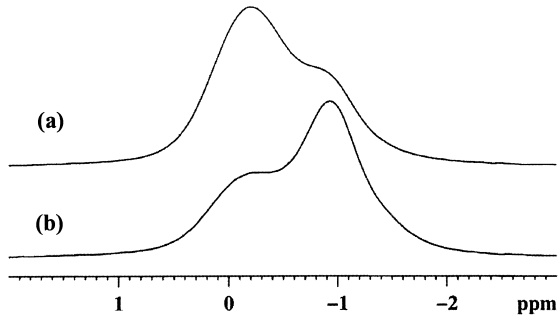

Fig. 6. ^{7}Li proton-decoupled MAS NMR spectra of (a) PEGDE-D400·$LiClO_4$ and (b) PEGDE-D2000·$LiClO_4$ complexes at the concentration of $[O]/[Li^+] = 10$ and 213 K.

due to the higher donicity of the unpaired electron on nitrogen. The spectrum as shown in Fig. 6(b) exhibits approximate the same ^{7}Li chemical shift as that of site I in Fig. 5. Thus we suggest that site I is attributable to the Li^+ ions coordinated to nitrogen atoms. From the above-mentioned results of IR, DSC and ^{7}Li MAS solid-state NMR measurements, the structure model of the polymer electrolyte networks is proposed as shown in Scheme 2.

4.4. Ionic conductivity measurements

The ionic conductivity of all polymer electrolyte networks was determined by means of impedance spectroscopy using stainless steel as blocking electrodes in the temperature range from 15 to 85 °C. From the Z'' versus Z' plot, ionic conductivity values were calculated at each temperature from the intercept of the curve with real axis. Fig. 7 illustrates the temperature dependence of ionic conductivity of the PEGDE-D400 doped with various $LiClO_4$ concentrations. Variation of conductivity with temperatures in these polymer electrolyte networks is found to obey the Vogel–Tamman–Fulcher (VTF) relationship as follows, where the transport of charger carrier is considered to be coupled with the segmental motion of polymer host.

$$\sigma(T) = AT^{-1/2}\exp[-B/\kappa_B(T - T_0)]$$

where A is a constant proportional to the number of carrier ions, B is the pseudoactivation energy related to polymer segmental motion, κ_B is the Boltzmann constant, and T_0 is a reference temperature at which the configurational entropy of the polymer becomes zero and is close to the glass transition temperature.

Fig. 8 shows the $LiClO_4$ concentration dependence of ionic conductivity at various temperatures. It is apparently observed that a maximum conductivity was obtained at the concentration of $[O]/[Li^+] = 15$. The free volume theory is useful to clarify the ion transport mechanism and to understand the mobility of polymer segment. Use of free volume theory proposed by Cohen and Turnbull [17] to polymer electrolytes reveals that the average free volume of the polymer host is one of the determinants of ionic conductivity of the electrolytes. As the concentration of salt

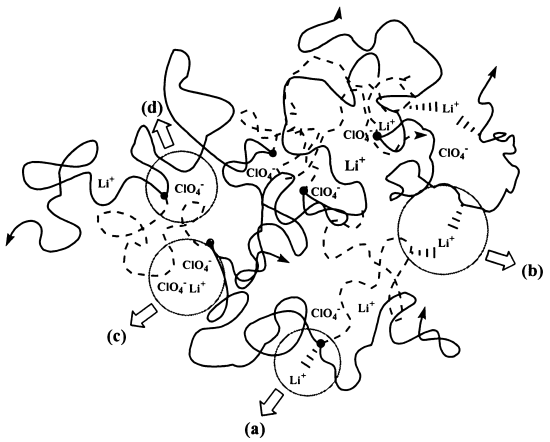

Scheme 2. Schematic representation proposed of crosslinked polymer electrolytes with different complexes formed by the interactions of (a) Li^+ with N, (b) Li^+ with polyether chains, (c) ion pairs or aggregates, and (d) hydrogen bonding clusters with ClO_4^- ions.

is increased, the number of charge carriers is also increased, but the average free volume is decreased due to the increase in T_g. At lower salt concentration level, the increase in the number of charge carriers dominates, and the decrease in free volume is compensated by the larger increase in the number of charge carriers. Hence, the conductivity is found to increase with $LiClO_4$ concentration at the lower concentration level. When the $LiClO_4$ concentration reaches at the concentration of $[O]/[Li^+] = 15$ or more, the decrease in free volume becomes more pronounced than the increase in number of charge carriers. At this time, the lower fraction of free volume is no longer compensated by the continuous increase in the number of charge carriers. Consequently, conductivity is decreased with the increase in salt concentration at higher $LiClO_4$ concentration level. Besides, the decrease in conductivity at higher salt concentrations is related to the other factors such as the formation of ion pairs

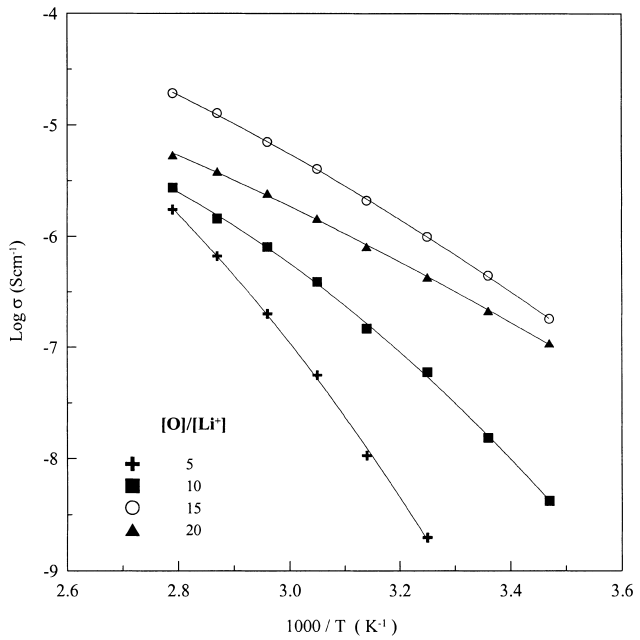

Fig. 7. Temperature dependence of ionic conductivity of PEGDE-D400·$LiClO_4$ complexes with various $LiClO_4$ concentrations.

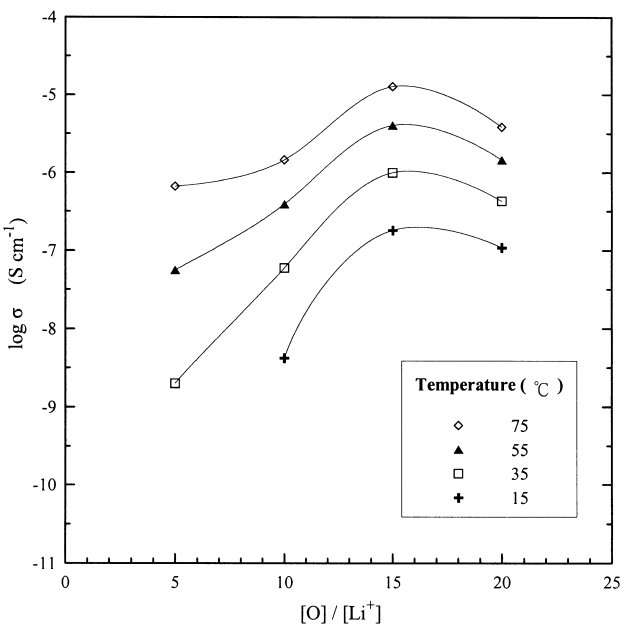

Fig. 8. Ionic conductivity as a function of $LiClO_4$ concentration of PEGDE-D400·$LiClO_4$ complexes at various temperatures.

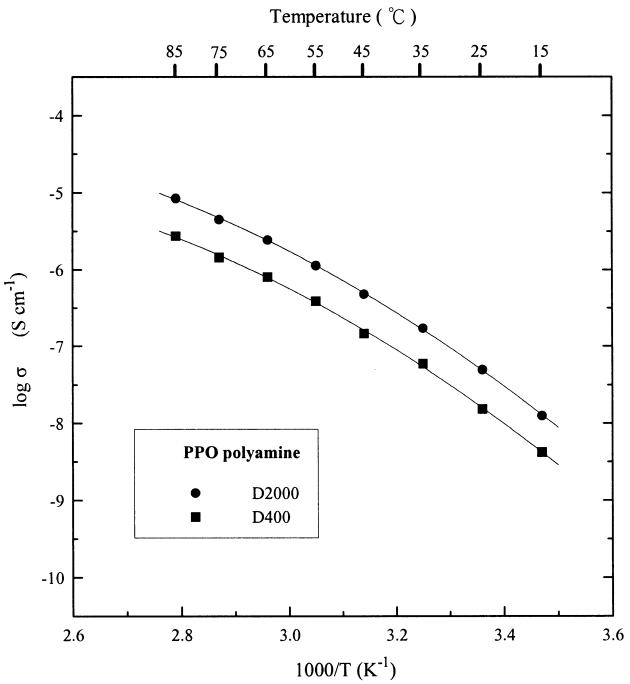

Fig. 9. Temperature dependence of ionic conductivity of PEGDE-D400·$LiClO_4$ and PEGDE-D2000·$LiClO_4$ complexes at the $LiClO_4$ concentrations of $[O]/[Li^+] = 10$.

and/or aggregates which tend to favor with increasing salt concentration. The formation of ion pairs or aggregates decreases the number density of charge carriers present, and also limit the mobility of the charge carriers throughout the polymer matrix; both effects results in a reduction in bulk ionic conductivity. These observations are consistent with the results from DSC and ^{7}Li MAS NMR spectroscopic studies.

Fig. 9 shows a comparison of the conductivity between PEGDE-D400·$LiClO_4$ and PEGDE-D2000·$LiClO_4$ complexes at the $LiClO_4$ concentrations of $[O]/[Li^+] = 10$. As is evident from Fig. 9, the ionic conductivities of the PEGDE-D2000·$LiClO_4$ complex are higher than those of the PEGDE-D400·$LiClO_4$ complex. This result can be ascribed to the T_{g1} (-15.3 °C, not shown) of PEGDE-D2000·$LiClO_4$ to be lower than that of the PEGDE-D400·$LiClO_4$ complex, and the lower T_{g1} of PEGDE-D2000·$LiClO_4$ complex results in the higher ionic mobility. This result demonstrates that the conductivity is affected by the ionic mobility, coinciding with the above-mentioned results of ^{7}Li solid-state NMR measurements.

5. Conclusions

A series of epoxide-crosslinked polyether networks doped/undoped with $LiClO_4$ have been characterized to be successfully prepared. On the basis of the results of FT-IR, DSC, TGA and ^{7}Li MAS solid-state NMR studies, new inter-chain interactions in these polymer complexes are found to be occurred due to the presence of hydrogen bonding clusters around ClO_4^- ions, and of the interactions between Li^+ ions and nitrogen atoms and between oxygen ligands of the polyether chains and the acceptor groups in these polymer networks. ^{7}Li NMR line shapes in these polymer complexes vary as a function of temperature and $LiClO_4$ concentration, and it is observed that the lithium mobility increases with the raising temperature, and the lithium cations are predominately coordinated to ether oxygen atoms subsequent to the nitrogen atoms of being saturated and are formed as ion pairs or aggregates under further addition of salt. The behavior of ion transport obeys the empirical VTF type relationship for all the samples, implying the diffusion of charge carrier is assisted by the segmental motions of polymer chains, and moreover the maximum ionic conductivity occurs at the $LiClO_4$ concentration of $[O]/[Li^+] = 15$.

Acknowledgements

The authors would like to thank the National Science Council, Taipei, ROC for their generous financial support of this research.

References

[1] MacCallum JR, Vincent CA, editors. Polymer electrolyte reviews, vols. 1 and 2. London: Elsevier; 19871989.
[2] Gray FM. Solid polymer electrolytes—functional and technological applications. Weinheim, Germany: VCH; 1991.
[3] Scrosati B. Application of electroactive polymers. London: Chapman and Hall; 1993.
[4] Acosta JL, Morales E. J Appl Polym Sci 1996;60:1185.
[5] Bruce PG, editor. Solid state electrochemistry. Cambridge: Cambridge University Press; 1997. p. 106.
[6] Berthier C, Gorecki W, Minier M, Armand MB, Chabagno JM, Rigaud P. Solid state ionics 1983;11:91.
[7] Fauteux D, Purd'homme J, Harvey PE. Solid state ionics 1988;28:923.
[8] Kuo PL, Liang WJ, Lin CL. Macromol Chem Phys 2002;203:230.
[9] Chen CC, Liang WJ, Kuo PL. J Polym Sci, Polym Chem Ed 2002;40:486.
[10] Liang WJ, Kuo CL, Lin CL, Kuo PL. J Polym Sci, Polym Chem Ed 2002;40:1226.
[11] Cohen H. J Chem Soc 1952;4282.
[12] Symons MCR. In: Kevan L, Webster BC, editors. Electron–solvent and ion–solvent interactions. New York: Elsevier; 1976. p. 311–41.
[13] Ochi M, Ozazaki M, Shimbo M. J Polym Sci, Polym Phys Ed 1982;20:689.
[14] Pogany GA. Polymer 1970;1:66.
[15] Enns JB, Gillham JK. J Appl Polym Sci 1983;28:2567.
[16] Lin CL, Kao HM, Wu RR, Kuo PL. Macromolecules 2002;35:3083.
[17] Cohen MH, Turnbull D. J Chem Phys 1959;31:1164.